Electrical signal-to-noise ratio improvement in indirect detection of mid-IR signals by wavelength conversion in silicon-on-sapphire waveguides

Y. Huang, E. K. Tien, S. Gao, S. K. Kalyoncu, Q. Song, F. Qian, E. Adas, D. Yildirim, and O. Boyraz[a)]
EECS Department, University of California, Irvine 92697, USA

(Received 4 June 2011; accepted 12 September 2011; published online 3 November 2011)

Planar waveguide devices based on silicon-on-sapphire are emerging as a bridge between mid-infrared (IR) and near-IR wavelength through frequency conversion process. We analyze the limits of indirect detection of mid-IR signals by wavelength conversion in such waveguides and investigate signal-to-noise ratio improvement that is attainable with respect to direct detection using state of the art commercial detectors. Our calculation shows that, in addition to room temperature and high speed operation, the proposed indirect detection can improve the electrical signal-to-noise ratio up to 40 dB compared to direct detection by PbSe, HgCdTe, and InSb detectors, especially in detection of weak mid-IR signals. © *2011 American Institute of Physics*. [doi:10.1063/1.3651292]

Mid-infrared (Mid-IR) spectral range is the window for a wide variety of applications, including free space communication, thermal and biomedical imaging, optical sensing, chemical spectroscopy and missile guidance/countermeasures. To facilitate these applications, efficient light detection is necessary. Mid-IR detectors are extremely limited in terms of operation condition, noise performance and speed.[1] A high-speed and compact solution for low-noise detection is still on-demand. Wavelength up-conversion can be utilized to solve the mid-IR light detection problem.[2] And waveguide-based wavelength converters can provide a chip-scale integrated solution with high effective nonlinearity due to high optical confinement. However, the mature silicon-on-insulator (SOI) waveguide technology meets its limitation in mid-IR due to high substrate loss. Silicon-on-sapphire (SOS) waveguides are considered as a good mid-IR alternative, because sapphire has a transparency window up to 6 μm and SOS waveguides are compatible with SOI technology.[3] Recently, we proposed a frequency band converter based on SOS waveguide capable of converting selected band of mid-IR signals to near-IR (1.55 μm).[4] Based on the converter, here, we propose an indirect detection scheme for mid-IR signal by using near-IR detectors. Since detectors at near-IR wavelengths exhibit superior performances in speed, noise, and sensitivity, the indirect detection scheme is promising to improve the detection performance.

In this letter, we analyze the limits of indirect detection of mid-IR signals by frequency band conversion in SOS waveguides and investigate its signal-to-noise-ratio (SNR) improvement with respect to direct detection using state-of-the-art commercial detectors. In particular, we provide a comparative study on the noise performance in detection of 4 μm mid-IR signals by using PbSe, HgCdTe, and InSb mid-IR detectors, and InGaAs photodetectors following a SOS channel waveguide based wavelength converter. We show that the proposed indirect detection can improve the electrical SNR (eSNR) up to 40 dB with respect to direct detection, where the improvement is more pronounced in detection of weak incident signals.

The upper branch in Figure 1 illustrates the indirect detection of mid-IR signals up-converted to near-IR wavelengths and detected by telecommunication detectors. Here, the wavelength conversion is generated through four-wave-mixing (FWM) based modulational instability at SOS waveguides.[4] Dispersion engineering on waveguides can alter the dispersion curve to meet the phase-matching condition for different mid-IR signal wavelengths. Low positive residual dispersion can be compensated by nonlinear phase shift and low phase mismatch produces exponential growth in parametric gain.[4,5] Figure 2(a) shows the conversion efficiency from mid-IR to telecommunication wavelength that can be achieved in different waveguide geometries calculated by numerically solving nonlinear Schrödinger equation.[4,6] It is possible to convert mid-IR signal between 4 μm and 6 μm to near-IR wavelengths of 1.55 μm by varying the width. The dark region in the figure corresponds to the pump wavelength region to enable the conversion from the peaked mid-IR to telecommunication wavelength. Thulium-doped fiber lasers and Chromium-based solid-state lasers can provide adequate pumping in this region.[7] Figure 2(b) shows the conversion efficiency and peak signal wavelength dependence on pump intensity, which shows optical pump saturation.[4]

Noise in indirect detection may originate from wavelength conversion process or the detector itself. Noise associated with wavelength conversion includes quantum noise, Raman induced noise, and pump transferred noise. Since the frequency separation is more than three times wider than the Raman shift in silicon, the Raman induced noise is negligible. Also, the noise transfer from pump is considered to be

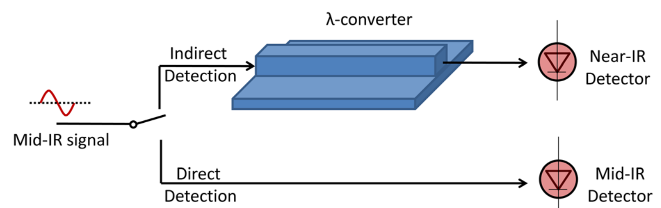

FIG. 1. (Color online) Schematics of direct and indirect mid-IR detection.

[a)]Author to whom correspondence should be addressed. Electronic mail: oboyraz@uci.edu.

 © 2011 American Institute of Physics

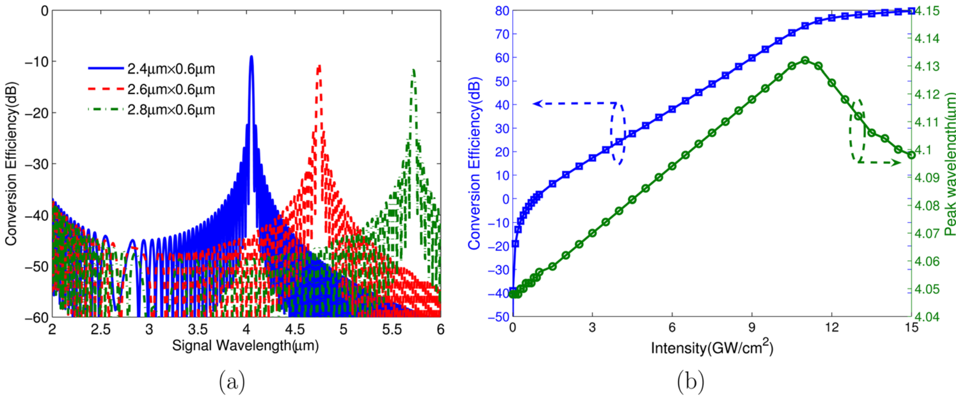

FIG. 2. (Color online) (a) Conversion efficiency from mid-IR to telecommunication wavelength. The dark region in the figure corresponds to the pump wavelength region to enable the conversion from the peaked mid-IR to telecommunication wavelength. The pump wavelength is greater than the 2.2 μm two-photon-absorption (TAP) threshold. (b) Conversion efficiency (blue) and peak wavelength (green) dependence on pump intensity.

detrimental for large signal powers, pump lasers with relative intensity noise (RIN) > 120 dB/Hz and large phase noise.[8,9] Since the noise performance of mid-IR pump lasers is not well characterized, we intentionally exclude the noise originating from the pump lasers in our calculations. However, excess quantum noise is always present in the parametric process and will be transferred to InGaAs-based p-i-n detector as quantum fluctuations, $i^2_{n,qt}$, described as[8]

$$i^2_{n,qt} = 4R^2 G_i P_{in} \frac{hv}{2}(2G_i + 1)B_e. \quad (1)$$

Here, R is responsivity of the detector, B_e is electrical bandwidth, P_{in} is incident power, and G_i is conversion efficiency. Other detector noise components in the InGaAs detector include thermal noise $i^2_{n,th}$ and shot noise $i^2_{n,sh}$ as in Eqs. (2) and (3), in which R_L is load resistance and F_n is the circuitry noise figure,[10]

$$i^2_{n,th} = 4(k_b T/R_L)F_n B_e, \quad (2)$$

$$i^2_{n,sh} = 2q(RP_{in} + i_d)B_e. \quad (3)$$

Lower arm in Figure 1 illustrates the direct detection of mid-IR signals. Commercial mid-IR detectors include photoconductive (PC), photovoltaic (PV), and thermal detectors. Thermal detectors are too slow for real-time application, and only PC and PV detectors are analyzed here. PV detectors absorb photons with energy beyond and near their bandgap to generate current. Because the bandgap for mid-IR detection is narrow, thermal generation can result in considerable dark current. Low temperature operation is always necessary to suppress dark current and the associated shot noise. The noise components in PV detectors include thermal noise, shot noise, and flicker noise. If a low-pass filter is inserted to eliminate flicker noise, the total noise $i^2_{n,pv}$ will mainly consist of thermal noise $i^2_{n,th}$ and shot noise $i^2_{n,sh}$ as in Eqs. (2) and (3).

TABLE I. Detector parameters used in calculation.

	T (K)	λ_{op} (μm)	R	R_L (Ω)	I_d	NEP (W/Hz$^{1/2}$)
InGaAs	300	1.55	0.95 (A/W)	8 M	80 pA	2×10^{-15}
PbSe	300	4.0	3×10^3 (V/W)	0.3 M	N/A	8×10^{-11}
HgCdTe	293	4.0	3×10^3 (V/W)	1 K	N/A	3.1×10^{-12}
InSb	77	4.0	2.5 (A/W)	1 M	10 μA	5.5×10^{-13}

In PC mode, photo-generated carriers change the conductivity of the medium and lead to a change on the voltage across the medium. Main noise components in PC detectors include thermal noise, generation-recombination noise (GR-noise), background noise, flicker noise, and noise transferred from voltage supply. While supply voltage induced noise can be minimized to negligible level by using low noise voltage supplies and flicker noise can also be eliminated by low-pass filters, the total noise $i^2_{n,pc}$ mainly includes thermal noise $i^2_{n,th}$, GR-noise $i^2_{n,gr}$, and background noise $i^2_{n,bg}$,[11,12]

$$i^2_{n,gr} = \int_0^{B_e} \frac{4qI_0\Gamma_G}{(1 + 4\pi^2 f^2 \tau^2)} df = \frac{2qI_0\Gamma_G}{\pi\tau}\tan^{-1}(2\pi B_e \tau), \quad (4)$$

$$i^2_{n,bg} = q^2 \eta A E_{BB} B_e, \quad (5)$$

where τ is average carrier lifetime, I_0 is the total generation current, Γ_G is the current gain, η is quantum efficiency, A is active detector area, $E_{BB} = \int_0^{\lambda_c} \varepsilon_\lambda \frac{2\pi c}{\lambda^4}\left[\frac{1}{e^{hc/\lambda k_b T} - 1}\right] d\lambda$ is the total photon flux density with λ_c being the cut-off wavelength, and ε_λ the emissivity for the window material.

To assess the detection limit and evaluate noise performance, we used state-of-the-art commercial mid-IR and near-IR photodetectors in our calculation. In particular, we use an InGaAs p-i-n detector for near-IR detection in the indirect scheme. For direct mid-IR detection, three types of detectors are widely used: InSb PV, PbSe PC, and HgCdTe PC detectors. While PbSe and HgCdTe detectors can work properly at

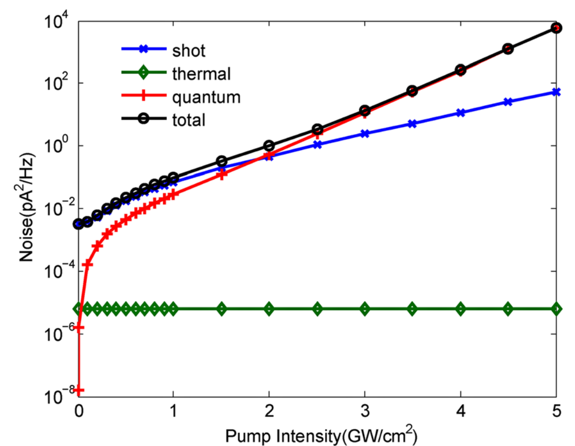

FIG. 3. (Color online) Detection noise at near-IR InGaAs detector in indirect detection.

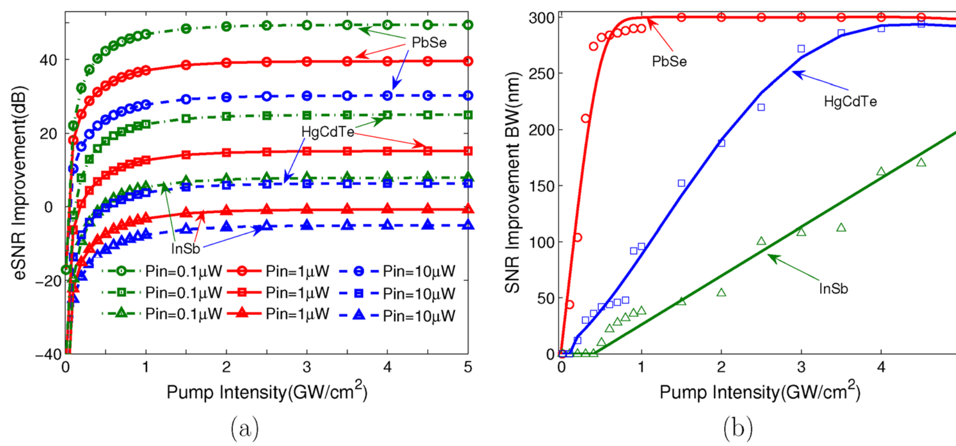

FIG. 4. (Color online) (a) eSNR improvement by using indirect detection with respect to direct detection. PbSe and HgCdTe photoconductive detectors are set to operate at room temperature and InSb photovoltaic detector is liquid nitrogen cooled to 77 K. (b) Bandwidth on which there is SNR improvement by using indirect detection increase almost linearly with intensity after the threshold and before saturation (Pin = 0.1 μW).

room temperature, InSb detectors usually require liquid-nitrogen or multi-stage TE cooling. Their main parameters are listed in Table I, which tracks the up-to-date commercial detectors, e.g., Hamamatsu and Vigo.[1,13] An electrical bandwidth of 0.1 MHz is used to accommodate the relatively slow mid-IR detectors. Figure 3 illustrates the noise at InGaAs detector after the wavelength-converter at room temperature with incident power level of 1 μW. At low pump intensities, the detection system will be limited by shot noise. As pump intensity increases above 0.4 GW/cm^2, the conversion efficiency increases and the quantum noise becomes dominant. Thermal noise is minor and cooling of near-IR detector cannot further improve the noise performance in indirect detection.

For direct detection at mid-IR, thermal noise dominates in PbSe and HgCdTe detectors and shot noise is the dominant noise in the liquid nitrogen cooled InSb detectors. We estimate that for the same 1 μW input power level at mid-IR the total noise current in PbSe, HgCdTe, and InSb detectors to be 0.10 $pA/\sqrt{Hz}$, 4.09 $pA/\sqrt{Hz}$, and 1.63 $pA/\sqrt{Hz}$, respectively.

To assess the noise improvement through indirect detection, we estimate the eSNR of detectors at three different incident mid-IR power levels of 0.1 μW, 1 μW, and 10 μW. The eSNR enhancement is evaluated by comparing the eSNR results of three mid-IR detectors to that of the InGaAs detector as: $eSNR_{near-IR}/eSNR_{mid-IR}$, as illustrated in Figure 4(a). At 1 μW, liquid nitrogen cooled InSb detectors can achieve about the same eSNR as indirect detection at 1550 nm. Indirect detection can provide >10 dB and >35 dB eSNR improvements over direct detection using HgCdTe and PbSe detectors, respectively. The eSNR improvement in these detectors is achieved for pump intensities above 0.1 GW/cm^2 at which conversion efficiency exceeds −20 dB. At the pump intensities below 1 GW/cm^2, the indirect detection will be limited by thermal and shot noised, and eSNR increases with increasing conversion efficiency. However, at pump intensities above 1 GW/cm^2, the indirect detection will be limited by the quantum noise of the parametric process, and the eSNR improvement will saturate at 40 dB level with respect to PbSe detector for 1 μW input power. The advantage of indirect detection will be more obvious for low input power levels. For instance, the SNR improvement with respect to PbSe can go up to 50 dB for 0.1 μW input power levels. Moreover, we even expect that indirect detection can provide 7 dB eSNR improvement with respect to liquid nitrogen cooled InSb detectors at such low power levels.

We also calculate the bandwidth on which indirect detection achieves better eSNR than direct mid-IR detection. As Figure 4(b) illustrates, we can attain eSNR improvements within up to 300 nm, 200 nm conversion bandwidths centered at 4 μm for input power levels of 0.1 μW with respect to PbSe and InSb detectors, respectively. Although the quantum noise saturates the eSNR improvement at the peak conversion wavelength, eSNR improvement bandwidth increases with increasing pump intensity. This is consistent with the tendency on conversion bandwidth increase with increasing pump intensity.[14]

In summary, indirect detection shows better eSNR performance at low incident power. At higher incident power, although liquid nitrogen cooled InSb PV detectors can achieve better SNR, indirect detection is still desirable for high-speed and room-temperature applications. The indirect detection scheme provides a solution for high speed processing of mid-IR signal with good noise performance, which can potentially drive the integration of photonic and electric IC.

This research was supported by DARPA Young Faculty Award, #66001-10-1-4036 and EU PIRG07-GA-2010-268370 grant.

[1] *Characteristics and Use of Infrared Detectors* (Solid State division, Hamamatsu Photonics K.K, Tokyo, Japan, 2004).
[2] K. Karstad, A. Stefanov, M. Wegmuller, H. Zbinden, N. Gisin, T. Aellen, M. Beck, and J. Faist, Opt. Lasers Eng. **43**, 537 (2005).
[3] R. A. Soref, S. J. Emelett, and W. R. Buchwald, J. Opt. A, Pure Appl. Opt. **8**, 840 (2006).
[4] E.-K. Tien, Y. Huang, S. Gao, Q. Song, F. Qian, S. K. Kalyoncu, and O. Boyraz, Opt. Express **18**, 21981 (2010).
[5] M. N. Islam and O. Boyraz, IEEE J. Sel. Top. Quantum Electron. **8**(3), 527 (2002).
[6] G. P. Agrawal, *Nonlinear Fiber Optics*, 4th ed. (Academic, San Diego, CA, 2007).
[7] R. Paschotta, *Encyclopedia of Laser Physics and Technology* (Wiley, Weinheim, Germany, 2008).
[8] P. Kylemark, P. O. Hedekvist, H. Sunnerud, M. Karlsson, and P. A. Andrekson, J. Lightwave Technol. **22**, 409 (2004).
[9] S. Moro, A. Peric, N. Alic, B. Stossel, and S. Radic, Opt. Express **18**, 21449 (2010).
[10] G. P. Agrawal, *Fiber-Optic Communication Systems*, 3rd ed. (Wiley, New York, 2002).
[11] S. Nudelman, Appl. Opt. **1**, 627 (1962).
[12] P. Bhattacharya, *Semiconductor Optoelectronic Devices* (Prentice-Hall, Englewood Cliffs, NJ, 1994).
[13] IR Detectors Catalogue (Vigo System, Ozarow Mazowiecki, Poland, 2006).
[14] R. H. Stolen and J. E. Bjorkholm, IEEE J. Quantum Electron. **QE-18**, 1062 (1982).